



# Characterization of chicken *IFI35* and its antiviral activity against Newcastle disease virus

Yan Qing JIA<sup>1)</sup>, Xiang Wei WANG<sup>2)</sup>, Xi CHEN<sup>2)</sup>, Xin Xin QIU<sup>1)</sup>, Xing Long WANG<sup>2)\*</sup> and Zeng Qi YANG<sup>2)\*</sup>

<sup>1)</sup>Department of Animal Engineering/Engineering Research Center of Animal Disease Prevention and Control, Universities of Shaanxi Province, Yangling Vocational & Technical College, Shaanxi Province, PR China

<sup>2)</sup>College of Veterinary Medicine, Northwest A&F University, Shaanxi Province, PR China

**ABSTRACT.** Interferon-induced protein-35 kDa (*IFI35*) was an antiviral protein induced by interferon (*IFN*)- $\gamma$ , which plays an important role in the *IFN*-mediated antiviral signaling pathway. Here, we cloned and identified *IFI35* in the chicken for the first time. Chicken *IFI35* (*chIFI35*) contains an open reading frame (ORF) of 1,152 bp encoding a protein of 384 amino acids containing two conserved *Nmi/IFI35* domain (NID) motifs. Tissue distribution analysis of *chIFI35* in healthy and Newcastle disease (ND) virus-infected chickens indicated a positive correlation between *chIFI35* mRNA transcription and ND viral loads in various tissues. The role of *chIFI35* in regulation NDV replication were further assessed by up- or down-regulated *chIFI35* expression in DF-1 cells transfected with plasmid harboring *chIFI35*, pCMV-3HA-*chIFI35* or shRNA targeting *chIFI35*, pshRNA-*chIFI35* plasmids. NDV replications in DF-1 cells were significantly reduced or slightly increased by over- or under-expression of the *chIFI35* protein, respectively, indicating the role of *chIFI35* in anti-NDV infection. Moreover, *chIFI35* also involved in regulation of viral gene transcription and *IFNs* expression. The collected data were meaningful for research of chicken antiviral immunity and shed light on the pleiotropic antiviral effect of *chIFI35* during NDV infection.

**KEY WORDS:** antiviral, chicken, interferon, interferon-induced protein-35 kDa, Newcastle disease virus

*J. Vet. Med. Sci.*

84(3): 473–483, 2022

doi: 10.1292/jvms.21-0410

Received: 22 July 2021

Accepted: 14 January 2022

Advanced Epub:

9 February 2022

Interferon-induced protein-35 kDa (*IFI35*), also known as IFP35, was one of the antiviral proteins induced by both type I and type II interferons (*IFNs*) [1]. *IFI35* was originally identified in 1994 as an *IFN*-induced protein by screening a cDNA library from HeLa cells treated with *IFN*- $\gamma$  [1]. It was widely expressed in various cells, such as fibroblasts, mononuclear macrophages, and epithelial cells, and its expression in the mitochondrial/lysosomal or microsomal fractions was increased by *IFN* treatment [1, 4]. This protein could translocate to the nucleus from the cytoplasm upon *IFN* stimulation. The protein interacts with N-Myc interacting protein (*Nmi*) and casein kinase 2 interacting protein-1 (*CKIP-1*), and which regulate the stability of *IFI35* [17, 28, 30]. Moreover, over-expression of *IFI35* could efficiently inhibit the replication of bovine foamy virus, prototype foamy virus [21], and foot-and-mouth disease virus [29], however, *IFI35* promoted vesicular stomatitis virus and Senda virus proliferation through degradation of retinoic acid inducible-gene I (*RIG-I*) suppressing the expression of *IFNs* [5]. *IFI35* has also been reported involving in various diseases, such as Sezary syndrome, which it was significantly down-regulated in patients, suggesting a role of it in suppression tumor [19]. To our knowledge, the pleiotropic effects of *IFI35* have not been examined in birds, besides limited reports about mammals and fish [5, 18, 29].

Newcastle disease (ND), one of the most highly contagious and infectious diseases, was causing serious death and economic losses in both domestic and wild avian species [20]. Newcastle disease virus (NDV), the causative agent of ND, belongs to the order Mononegavirales, family Paramyxoviridae and genus *Avulavirus* [24]. The etiology of the disease was the velogenic strains of NDV, including viscerotropic and neurotropic velogenic NDV strains [11]. NDVs were identified to be excellent inducer of *IFNs*, while they gain potent immunosuppressive ability through evolution [9, 16]. NDVs regulated *IFNs* expression have been identified through impact key elements, like *MDA5*, *STAT*, in *IFN* pathway [13, 25]. While, there will be a series of steps before we completely reveal these mechanism involving in the host-virus interactive stages during NDV infection. Especially, the functions

\*Correspondence to: Yang, Z. Q.: yzq8162@163.com; Wang, X. L.: wxlong@nwsuaf.edu.cn, College of Veterinary Medicine, Northwest A&F University, Yangling, Shaanxi Province 712100, PR China

©2022 The Japanese Society of Veterinary Science



This is an open-access article distributed under the terms of the Creative Commons Attribution Non-Commercial No Derivatives (by-nc-nd) License. (CC-BY-NC-ND 4.0: <https://creativecommons.org/licenses/by-nc-nd/4.0/>)

of most downstream molecules in chicken *IFN* pathways, including *IFI35*, *OASL*, and *Mx*, are still not clear. In our previous study, *IFI35* was significantly up-regulated in velogenic NDV-infected chicken visceral tissues using transcriptome sequencing compared with lentogenic NDV or control-infected chicken tissues. Here, the molecular characterization of chicken *IFI35* (*chIFI35*) and its antiviral role in against NDV infection were analyzed in the current study.

## MATERIALS AND METHODS

### *Animals, cells, and virus*

The specific pathogen free (SPF) chicken embryonated eggs were purchased from the Merial-vital Laboratory Animal Technology (Beijing, China). Nine-day-old SPF chicken embryos were incubated at 37°C for viral amplification or making chick embryo fibroblast (CEF) cells. The SPF chickens were fed in isolator until 21 days old for experiments.

All incubations and reactions were performed under 5% CO<sub>2</sub> and 37°C in flat-bottom plates. DF-1, CEF, and HEK293T cells were maintained and cultured in Dulbecco's modified Eagle's medium (DMEM, Gibco, Grand Island, NY, USA) with 10% fetal bovine serum (FBS, Hyclone, Logan, UT, USA).

NDV strains, velogenic strain F48E9, and lentogenic strain rLa Sota-GFP were obtained from Northwest A&F University Infectious Diseases Lab. Viruses were propagated in 9-day-old SPF chicken embryonated eggs, titrated with the hemagglutination (HA) test, and then stored at -80°C for further use.

### *RNA extraction and cDNA preparation*

Total RNA was extracted using Trizol (TaKaRa, Dalian, China) according to the instructions. The cDNA was synthesized using StarScript II First-Strand cDNA Synthesis Mix (GenStar, Beijing, China) according to the instructions. In brief, the reaction was performed in a volume of 20 µl, contained 500 ng total RNA, 10 µl 2 × Reaction mix, 1 µl oligo (dt)<sub>18</sub> (50 µM), 1 µl StarScript II RT Mix, and RNase-free ddH<sub>2</sub>O up to 20 µl. Each reaction used the following conditions: 25°C for 10 min, 42°C for 30 min, and 85°C for 5 min. The resultant cDNA was stored at -20°C for further use.

### *Cloning, sequencing, and bioinformatic analysis of chIFI35 sequences*

The primers of the partial sequence of *chIFI35* including the full-length ORF were designed based on the computer-predicted sequence of *Gallus gallus IFI35* and our transcriptome data of chicken visceral tissues (data not shown). Primers are listed in Table 1. The amplification was performed as follows: initial denaturation at 95°C for 5 min followed by 35 cycles at 95°C for 30 sec, annealing at 55°C for 30 sec and extension at 72°C for 30 sec, and a further extension at 72 for 10 min following the last cycle. The PCR products were purified and cloned into the pMD19-T vector (TaKaRa, Dalian, China), and then sent to Genweizhi (Suzhou, China) for sequencing.

The sequence and protein were analyzed as previous described [18, 25–27]. In brief, the potential open reading frame (ORF) and homology search of *chIFI35* were analyzed by the ORF finder ([www.ncbi.nlm.nih.gov/gorf/gorf.html](http://www.ncbi.nlm.nih.gov/gorf/gorf.html)) and BLAST program (<http://blast.ncbi.nlm.nih.gov/Blast.cgi>) in NCBI. Protein molecular weight, isoelectric point, and instability index of *chIFI35* were predicted by the online server site ([www.sciencegateway.org/tools/proteinmw.htm](http://www.sciencegateway.org/tools/proteinmw.htm)) and the Prot-Param tool on ExPASy (<http://web.expasy.org/protparam/>), while the domains and motifs of *chIFI35* were determined using SMART (<http://smart.embl-heidelberg.de/>) and MotifScan ([http://myhits.isb-sib.ch/cgi-bin/motif\\_scan](http://myhits.isb-sib.ch/cgi-bin/motif_scan)). The MultiLoc tool (<http://abi.inf.unituebingen.de/Services/MultiLoc/>) predicted the cellular distribution of *chIFI35*, and SignalIP (<http://www.cbs.dtu.dk/services/SignalIP/>) and the SACS MEMSAT2 tool (<http://www.sacs.ucsf.edu/cgi-bin/memsat.py>) were used to analyze the signal peptide and transmembrane segments of *chIFI35*. Multiple sequence alignment was conducted using Clustal W 1.83, and the sequence diversity and phylogenetic analyzes were predicted using the MEGA 5.2 program.

### *Real-time quantitative PCR (RT-qPCR)*

RT-qPCR was used to detect the expression of mRNA of target genes using the 2 × RealStar Green Power kit (GenStar, Beijing, China) according to the manufacturer's instructions. Primers used in this study are listed in Table 1 [7, 12, 14]. The relative expression levels of the target genes were calculated using the 2<sup>-ΔΔCT</sup> method [15], and 28S was used to normalize the fold-changes in expression.

### *Tissue distribution profile of chIFI35 expression in vivo*

In order to investigate the tissue distribution of *chIFI35*, various tissues, including the blood, brain, bursa of fabricius, liver, spleen, heart, lung, intestines, pancreas, kidney, proventriculus, gizzard, trachea, skin, and muscle were collected from 21-day-old SPF chickens for RT-qPCR.

To evaluate the mRNA expression level of *chIFI35* in the tissues in NDV-infected chickens, the tissues that highly expressed *chIFI35* were collected from NDV-infected chickens and analyzed using RT-qPCR. In brief, 21-day-old SPF chickens were injected with 100 µl F48E9 (2<sup>8</sup> HA) and control birds were injected with 100 µl PBS (three chicken). At 24 hr post-infection, all chickens were euthanized, and the organs were collected and analyzed by RT-qPCR as above.

### *Expression plasmid construction and cell transfection*

To demonstrate the molecular function of *chIFI35 in vitro*, the full-length *chIFI35* sequence was cloned into the pCMV-3HA or

**Table 1.** The primers used in this study

Primers	Sequences (5'-3')	Methods	Size (bp)	References
<i>IRF1</i>	F: GCTACACCGCTCACGA R: TCAGCCATGGCGATT	RT-qPCR	133	[12]
<i>MAVS</i>	F: CCTGACTCAAACAAGGGAAG R: AATCAGAGCGATGCCAACAG	RT-qPCR	123	[7]
<i>STING</i>	F: TGACCGAGAGCTCCAAGAAG R: CGTGGCAGAACTACTTTCAG	RT-qPCR	63	[7]
<i>TBK1</i>	F: AAGAAGGCACACATCCGAGA R: GGTAGCGTGCAAATACAGC	RT-qPCR	152	[7]
<i>NF-<math>\kappa</math>b</i>	F: CATTGCCAGCATGGCTACTAT R: TTCCAGTCCCCTTCTTCAC	RT-qPCR	102	[7]
<i>IRF7</i>	F: CAGTGCTTCTCCAGCACAAA R: TGCATGTGGTATTGCTCGAT	RT-qPCR	169	The present study
<i>IFI35</i>	F: AGGGAGTTCCTGGATGAC R: GCTCCTCAGCCAGCACAT	RT-qPCR	229	The present study
<i>LGP2</i>	F: CCAGAATGAGCAGCAGGAC R: AATGTTGCACTCAGGGATGT	RT-qPCR	109	The present study
<i>MDA5</i>	F: TTGTCAGAGAGAGCAGTGTATTGGA R: GAATCACTGGTCGTGCTGCTGTGC	RT-qPCR	109	The present study
<i>IFN-<math>\alpha</math></i>	F: GACATGGCTCCCACTACC R: AGGCGCTGTAATCGTTGTCT	RT-qPCR	330	[14]
<i>IFN-<math>\beta</math></i>	F: TCCAGCTCCTTCAGAATACG R: TGCGGTCAATCCAGTGTT	RT-qPCR	192	The present study
<i>IFN-<math>\gamma</math></i>	F: TGAGCCAGATTGTTTCGATG R: CTTGGCCAGGTCCATGATA	RT-qPCR	134	[14]
<i>28S</i>	F: GGTATGGGCCCCGACGCT R: CCGATGCCGACGCTCAT	RT-qPCR	160	The present study
<i>NP</i>	F: TCGGATGAAAGGAGATAATGCG R: GTCTCCAGAATGATGTGCTCAT	RT-qPCR	182	The present study
<i>P</i>	F: CAATAAATCGTCCAATGCTAA R: CTCCATCATAGACATCATCGC	RT-qPCR	322	The present study
<i>M</i>	F: CCGATCGTCTACAAGACACAG R: GGACGCTTCTAGGCAGAGCAT	RT-qPCR	223	The present study
<i>F</i>	F: GACGGATTATCGCAACTAGCAG R: GCCGCTACCGATTAATGAGCTG	RT-qPCR	294	The present study
<i>HN</i>	F: CTACAGGATCAGGTTGCACTCG R: CCTGTTGAGATGTCCGAGCA	RT-qPCR	151	The present study
<i>L</i>	F: CCATTGGTCAAGCACAAACTAC R: GCCTTGTGAACAGTTCTCCATA	RT-qPCR	325	The present study
pCAGGS-Flag-ch <i>IFI35</i>	F: GGAATTCATGGACTCGGAGGAGGACTC R: GAAGATCTTCACTTATCGTGCATCCTTGTAATCGGGCTGGCCCATATCC	IFA	1,191	The present study
pCMV-3HA-ch <i>IFI35</i>	F: GGAATTCATGGACTCGGAGGAGGACTC R: GCTCTAGATCAGGGCTGGCCCATATCC	Coding region Amplification	1,167	The present study
<i>IFI35</i> -shRNA1	F: GATCCGCTGTAGAGCAGAGGTTACAATTCAAGAGATTGTAACCTCTGCTCTACAGCTTTTTTG R: AATTCAAAAAAGCTGTAGAGCAGAGGTTACAATCTTGAATTGTAACCTCTGCTCTACAGCG	Interference	63	The present study
<i>IFI35</i> -shRNA2	F: GATCCGGTAGTGTTTAAGGGACTTACTTCAAGAGAGTAAGTCCCTTAAACTACTCTTTTTTG R: AATTCAAAAAAGGTAGTGTTTAAGGGACTTACTTCTTGAAGTAAAGTCCCTTAAACTACTCCG	Interference	63	The present study
<i>IFI35</i> -NC	F: GATCCGCGATTGAAGCTTGTCTCTCATTTCAAGAGATAGCGAAGAAACCGATCTTGCTTTTTTG R: AATTCAAAAAAGCAAGATCGGTTTCTTCGCTATCTTGAATGAGAGACAAGCTTCAATCGCG	Interference	63	The present study

pCAGGS vector. Primers are listed in Table 1. Recombinant plasmids, including pCMV-3HA-ch*IFI35* and pCAGGS-Flag-ch*IFI35*, were confirmed by DNA sequencing. In order to test the effect of ch*IFI35* on NDV proliferation, we designed shRNA primers (*IFI35*-shRNA1, *IFI35*-shRNA2, and *IFI35*-NC) using the BLOCK-iT™ RNAi Designer (<https://rnaidesigner.thermofisher.com/rnaiexpress/design.do>), and the primer sequences are listed in Table 1. Next, double-stranded of shRNA was synthesized and cloned into the lentiviral expression plasmid pCD513B-U6-neo, which we named pCD513B-ch*IFI35*-shRNA1 (shRNA1), pCD513B-

ch $IFI35$ -shRNA1 (shRNA2), and pCD513B-ch $IFI35$ -negative control (NC). All the sequences of the plasmids were confirmed by sequencing. Other plasmids, including pCAGGS-Flag-ch $IFN-\alpha$ , pCAGGS-Flag-ch $IFN-\beta$ , and pCAGGS-HA- $P$  were previously constructed in our laboratory.

Cell transfection was carried out using Turbofect transfection reagent (Thermo Scientific, Waltham, MA, USA) according to the manufacturer's instructions. In brief, DF-1 cells were seeded in 24-well plates, and a mixture of Turbofect and plasmids was added, and then cultured at 5% CO<sub>2</sub> and 37°C.

#### Virus titration

Viral multiplications were quantified by the 50% tissue culture infection dose (TCID<sub>50</sub>) as previously described [6]. Briefly, DF-1 cells were seeded into 96-well plates for 24 hr. Virus supernatants from cell cultures were 10-fold serially diluted and then 100 µl/well were respectively added (three replicates) for infection. Five days after infection, the TCID<sub>50</sub> was calculated using Reed–Muench method.

#### Western blotting

Western blotting was used to analyze  $IFI35$  expression in DF-1 cells post-treatment. After transfected for 48 hr, cells were washed twice with PBS and lysed for 10 min by radio immunoprecipitation assay (RIPA) buffer with protease inhibitor Phenylmethylsulfonyl fluoride (PMSF) on ice. Cell lysate proteins were separated by 10% SDS-PAGE, blotted onto polyvinylidene difluoride (PVDF) membranes (Millipore, Boston, MA, USA), and subsequently probed with mouse anti- $HA$  monoclonal antibody and mouse anti- $GAPDH$  monoclonal antibody (CoWin Biosciences, Beijing, China) for 2 hr at room temperature to detect  $IFI35$  and  $GAPDH$ , respectively. HRP-conjugated goat anti-mouse IgG (Sungene Biotech, Shanghai, China) was used as a secondary antibody. Immunostained proteins were visualized using ECL peroxidase substrate (Millipore, Boston, MA, USA).

#### Immunofluorescence staining

DF-1 cells were grown to 50–60% confluence on coverslips and were co-transfected with the plasmids pCAGGS-HA- $P$  and pCAGGS-Flag-ch $IFI35$  for 36 hr. Cells were fixed in 4% paraformaldehyde for 30 min, permeabilized with 0.25% Triton X-100 for 15 min, and blocked with 30% bovine serum albumin (BSA) for 30 min. Next, cells were stained with anti-Flag and anti- $HA$  mAbs, followed by staining with secondary antibodies conjugated to Alexa Fluor 594 or fluorescein isothiocyanate (FITC; Sangon Biotech, Shanghai, China). Nuclei were stained with 4',6-diamidino-2-phenylindole (DAPI), and the colocalization of  $P$  protein and ch $IFI35$  were visualized using a Nikon CI-si confocal fluorescence microscope (Nikon Instruments Inc., Melville, NY, USA).

#### Statistical analysis

Experiments were repeated independently at least twice. GraphPad prism was used to statistical analysis. All data are showed as the mean ± standard error of the mean (SEM). The significant differences between two groups were performed using Student's  $t$ -tests in GraphPad software. The results were considered to be statistically significant as follows: \*\*\* $P$ <0.001, \*\* $P$ <0.01, \* $P$ <0.05, and ns mean not significant.

## RESULTS

#### Molecular and genetic character of ch $IFI35$

In our previous transcriptome study, we discovered that  $IFI35$  was up-regulated in both velogenic (F48E9) and lentogenic (La Sota) NDV infected groups, but the expression in F48E9 infected (5.34 fold-change) was much higher than La Sota infected (1.25 fold-change) using next-generation sequencing [10]. In this study, an 1,152 bp full-length ORF of  $IFI35$  was first amplified and cloned from chicken visceral tissue (ch $IFI35$ ). The obtained sequence (GenBank accession number: KY931454) has 99% similarity with computer-predicted *Gallus gallus*  $IFI35$  sequence (XM\_418132.5). Phylogenetic analysis based on the deduced amino acid sequences certified that  $IFI35$  was conserved among similar species but significant difference among different species (Fig. 1). Ch $IFI35$  was composed of 383 amino acids (Fig. 1A), with the theoretical isoelectric point of 5.14 and calculated molecular mass of 46.3 kDa. It was predicted unstable due to 51.59% instability probability, which indicated that this protein was unstable.

Ch $IFI35$  protein mainly distributed in the cytoplasm with cellular location prediction by MultiLoc tool. No putative signal peptide and trans-membrane region were found based on signal peptide analysis and trans-membrane domain prediction program. According to analysis with SMART software, the domain structure of the obtained ch $IFI35$  was similar to the predicted sequence (XM\_418132.5) and both composed of two characteristic Nmi/ $IFI35$  domains (NIDs) at positions 166–263 and 274–361.

Ch $IFI35$  sequence showed 89.2% identity to that from *Meleagris gallopavo* (avian), 47.9% from *Xenopus tropicalis* (amphibian), 44.5% from *Cynoglossus semilaevis* (fish), 52.5% from *Anolis carolinensis* (reptile), and 40.2% from *Mus musculus* (mammalian) (Table 2). Five clusters present in the Phylogenetic tree constructed based on the  $IFI35$  amino acid sequences from different species (Fig. 1B), and interestingly, the different taxa-derived  $IFI35$  counterparts formed separate sub-clusters that agreed with their orthodox taxonomy. Ch $IFI35$  belongs to the  $IFI35$  group of birds and has a close relationship with *Meleagris gallopavo*.

**Table 2.** Estimates of evolutionary divergence between chicken interferon-induced protein-35 kDa (*chIFI35*) and other species sequences

		Percent identity							
		1	2	3	4	5	6	7	8
Divergence	1		47.9	89.2	44.5	46.2	39.9	40.2	52.5
	2	86.9		47.4	45.7	46.3	39.8	41.1	49.0
	3	5.2	85.2		45.9	46.9	46.5	46.2	58.8
	4	92.4	100	88.3		62.3	36.6	36.4	44.9
	5	85.9	98.7	81.8	55.1		40.6	39.4	45.8
	6	75.9	92.2	74.3	103.1	79.5		84.0	45.9
	7	75.6	87.5	76.5	107.0	86.9	26.3		45.5
	8	65.1	81.5	63.5	99.3	92.5	79.8	82.8	

1–8 represent the species of *Gallus gallus*, *Xenopus tropicalis*, *Meleagris gallopavo*, *Cynoglossus semilaevis*, *Kryptolebias marmoratus*, *Homo sapiens*, *Mus musculus*, and *Anolis carolinensis*, respectively.

### Tissue distribution profile of *chIFI35* and transcriptional response against immune stimulation by NDV infection in SPF chicken

In the previous study of F48E9-infected chicken embryo (Fig. 2A, the allantoic cavity infection) or bursa of fabricius (Fig. 2B, Intramuscular injection) RNA sequencing, it was found that the expression of *IFI35* was significantly increased [10, 22]. In healthy SPF chickens, *chIFI35* mRNA had high level transcription in the lungs, glandular stomach, brain, bursa of fabricius, gizzard, kidney, heart, intestines, liver, and muscle, whereas, lower level expressed in the trachea, spleen, pancreas, and skin (Fig. 2C).

Velogenic NDV, F48E9, infection increased *chIFI35* expression in various immune-associated tissues of chickens (Fig. 2D). The highest level of *chIFI35* expression was detected in intestine, which also was one of the major target of NDV. The expressions of *chIFI35* in trachea, bursa of fabricius, and spleen were also significantly unregulated comparing with control group. Interestingly, high viral loads were detected in intestine, kidney, lung and brain, basically consistent with the high expression of *chIFI35*, which suggested that a certain correlation between *chIFI35* expression and NDV load in various tissues (Fig. 2E).

### *ChIFI35* plays an antiviral role against NDV infection in DF-1 cells

Over-expressed or down-expressed *chIFI35* in DF-1 cells transfected with plasmids were confirmed by western blotting assay at 24 hr post transfection (hpt) (Fig. 3A and 3D). NDV strains, F48E9 or rLa Sota-GFP, were used to infect the cells at 24 hpt. The proliferations of the virus in supernatants of different treated cells were quantified by testing viral TCID<sub>50</sub>. Comparing with the untreated cells, over-expressed *chIFI35* could significantly decrease F48E9 and rLa Sota-GFP propagation (Fig. 3B and 3C). However, viral proliferations in *IFI35*-down-regulated DF1 cells were slight enhanced with no significantly different (Fig. 3E and 3F). These data suggested that *chIFI35* has a certain antiviral ability.

### *ChIFI35* affects the transcription of RNA viral proteins

*IFI35* affect DNA virus transcription by interacts with one or more viral proteins. Whether it also plays a role in RNA virus replication has not been clearly illuminated. The distribution of *chIFI35* and NDV protein *P* were identified by co-transfected plasmids, pCAGGS-Flag-*chIFI35* and pCAGGS-HA-*P*, and the proteins of Flag-*chIFI35* and HA-*P* in cells were co-localization under laser confocal scanning microscopy (Fig. 4A). Furthermore, the transcription of different NDV genes in cell transfected empty vector or plasmids overexpressing of *chIFI35* were detected. The *CT* value of *P* gene was significant increased when over-expression of *chIFI35*, which indicated that *P* gene transcription was reduced at 12 hr after F48E9 infection. The transcription of *NP*, *P*, *F* and *HN* genes were also down regulated at 24 hr (Fig. 4B). Hence, these data indicated that *chIFI35* may inhibit NDV proliferation by affect NDV gene transcription, especially for *P* and *F*.

### *ChIFI35* enhances *IFN* expression

Since *IFI35* involved in *IFN* pathway, the correlation between *IFI35* and *IFNs*' expression were further analysis with RT-qPCR. Cells were collected at different time points after F48E9 infection, and then the expression of *chIFI35*, *IFN $\alpha$* , *IFN $\beta$* , and *IFN $\gamma$*  were detected. *ChIFI35* expression was keep increasing after NDV infection, which was similar to the *IFN $\alpha/\beta/\gamma$*  expression (Fig. 5A–D). The expressions of *IFN $\alpha/\beta/\gamma$*  in cells over-expressed *chIFI35* were also quantified. Over-expressed *chIFI35* could significantly enhanced type I and type II *IFNs* expression in cells (Fig. 5E). And interestingly, *chIFI35* was also significantly up regulated when *IFN $\alpha/\beta$*  were over-expressed in cells (Fig. 5F).

Furthermore, the expression of *IFNs* signaling pathway molecules, including *MDA5*, *LGP2*, *MAVS*, *STING*, *TBK1*, *IRF1*, *IRF7*, and *NF- $\kappa$ B*, were detected and compared in cells over- or normal- expressing *chIFI35* after F48E9 infection. The transcriptions of *MAVS*, *IRF7*, and *NF- $\kappa$ B* were not significant differently both in CEF and DF-1 cells, whereas *MDA5*, *LGP2*, *STING*, *TBK1*, and *IRF-1* were significantly increased (Fig. 6) when *chIFI35* was overexpressed, indicating that *chIFI35* play a role in promoting the expression of *IFNs*.

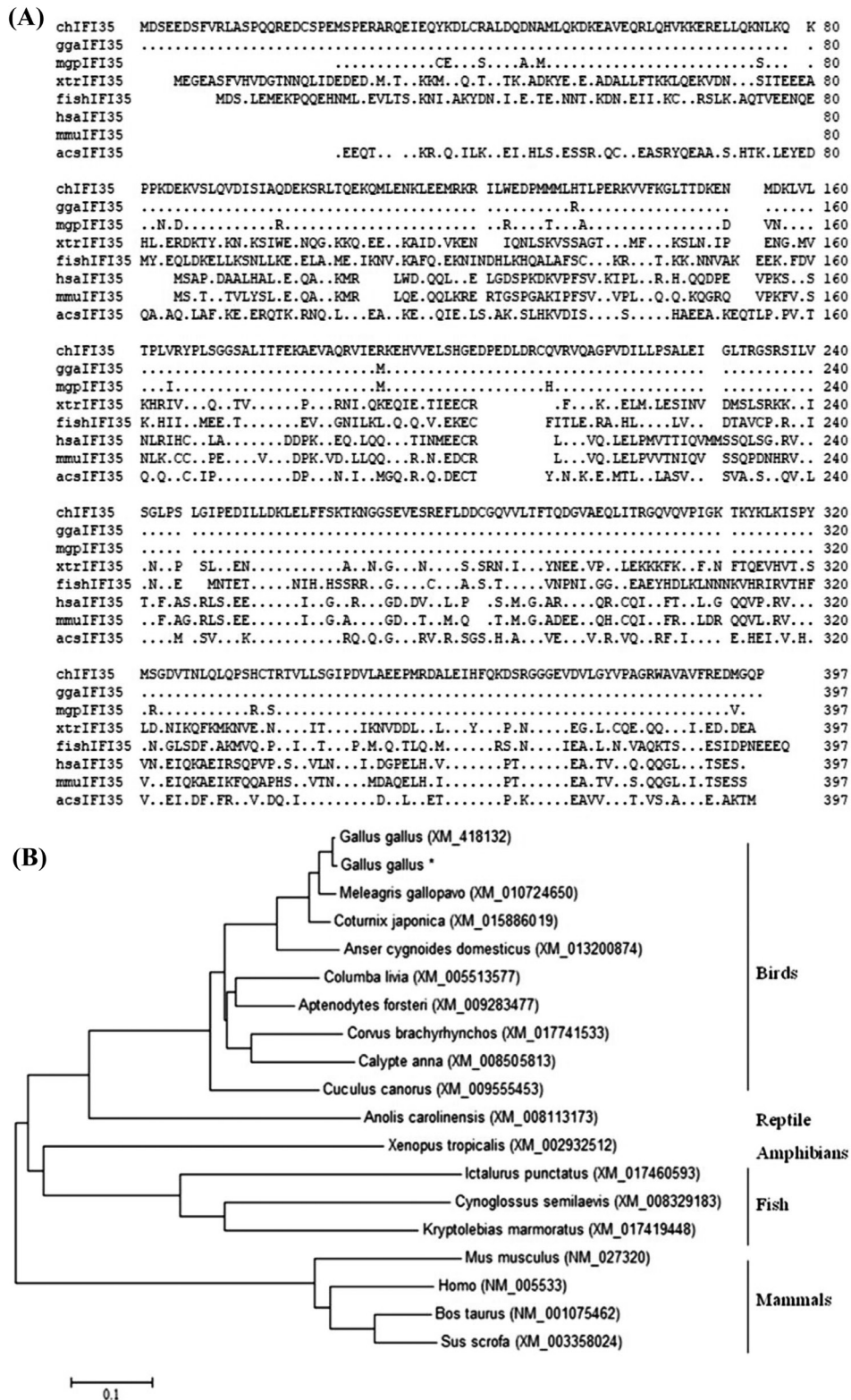


**Fig. 1.** Multiple alignment analysis and phylogenetic tree construction based on the interferon-induced protein-35 kDa (*IFI35*) amino acid sequences. (A) Multiple alignment analysis of *IFI35* family amino acid sequences using Clustal W in DNASTar. These sequences were downloaded from GenBank with accession numbers as follows: XM\_418132 (*Gallus gallus IFI35*, *ggaIFI35*), XM\_010724650 (*Meleagris gallopavo IFI35*, *mgpIFI35*), XM\_002932512 (*Xenopus tropicalis IFI35*, *xtrIFI35*), XM\_008329183 (*Cynoglossus semilaevis IFI35*, *fishIFI35*), NM\_005533 (*Homo IFI35*, *hasIFI35*), NM\_027320 (*Mus musculus IFI35*, *mmuIFI35*) and XM\_008113173 (*Anolis carolinensis IFI35*, *acsIFI35*). Amino acids conserved among species were indicated as identical “\*”. (B) Evolution analyzes were conducted using MEGA6.0. Numbers in branches indicate evolutionary distances. The evolutionary history was inferred using the neighbor-joining (NJ) method. The evolutionary distances were computed using the Poisson correction method.

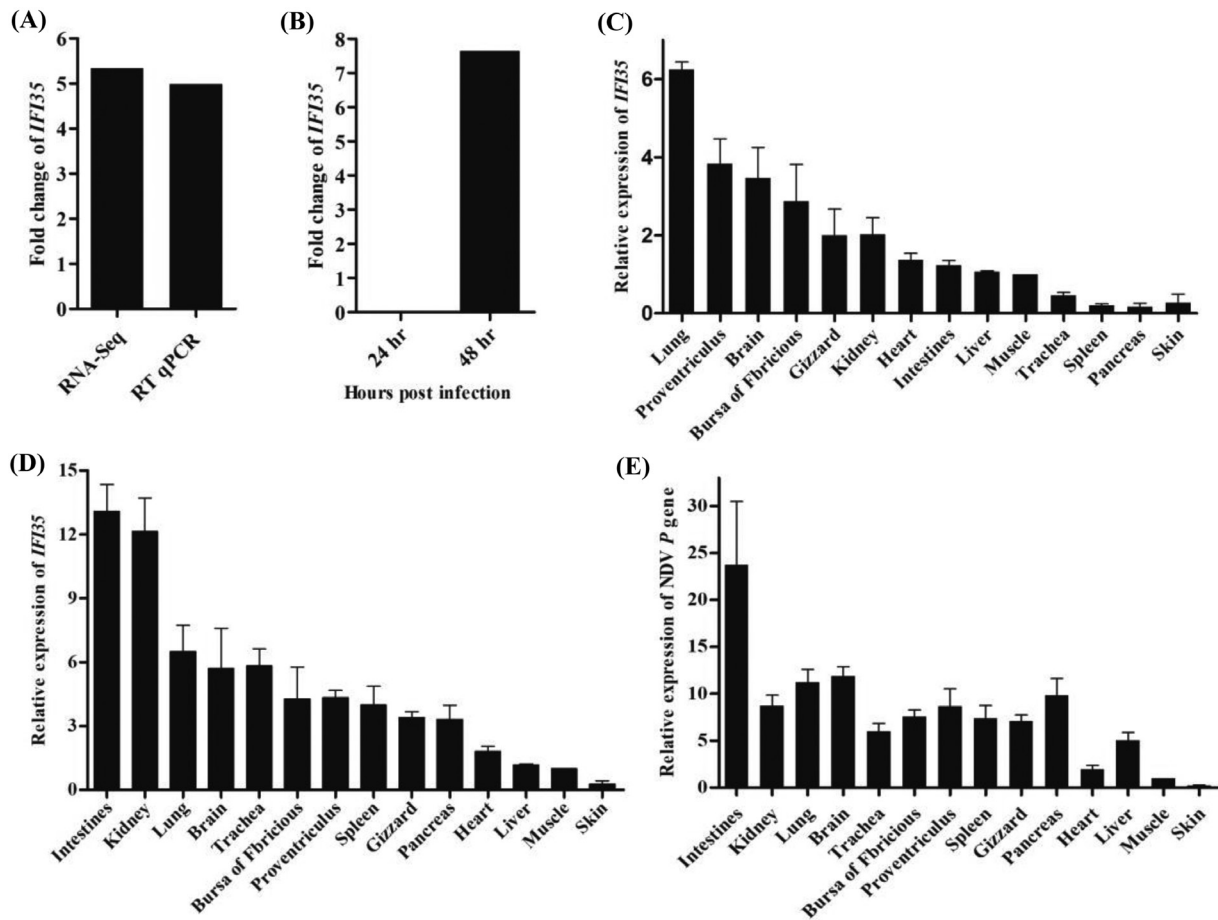


**Fig. 2.** Tissue distribution profile of chicken interferon-induced protein-35 kDa (*chIFI35*). The relative expression of *chIFI35* of F48E9 infected chicken embryo using RNA-Seq and RT-qPCR (A). The relative expression of *chIFI35* at 24 hr and 48 hr after F48E9 infected the bursa of fabricius (B). The tissue distribution profiles of *chIFI35* in various tissues in healthy chicken (C) and F48E9-infected chickens (D). (E) The viral loads of Newcastle disease virus (NDV) in different tissues.

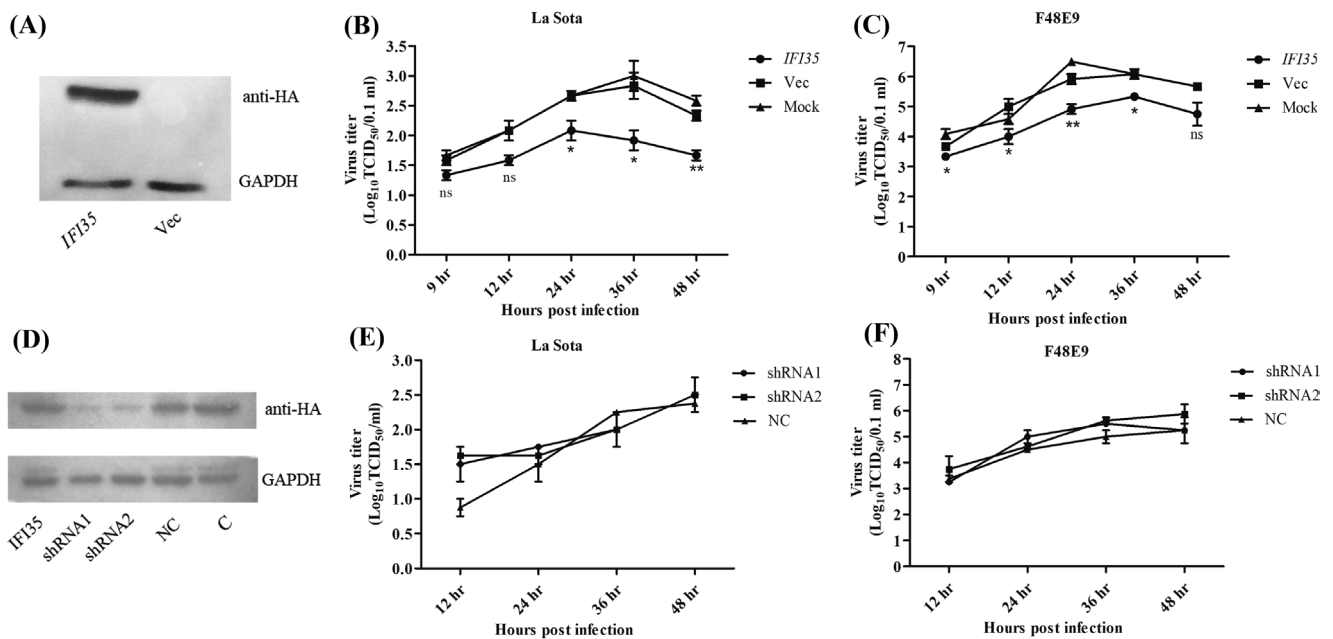


**Fig. 3.** Viral titers of Newcastle disease virus (NDV) in DF-1 cells with interferon-induced protein-35 kDa (*IFI35*) over- or under-expression. DF-1 cells were transfected with pCMV-3HA-*IFI35*, empty vector plasmids (A), or interference plasmids (D) for 24 hr, and infected with La Sota (1 moi) or F48E9 (0.1 moi). The viral titer of La Sota (B, E) and F48E9 (C, F) at different time points were detected using the TCID<sub>50</sub> method. \*\* $P < 0.01$ , \* $P < 0.05$ , and ns, not significant.

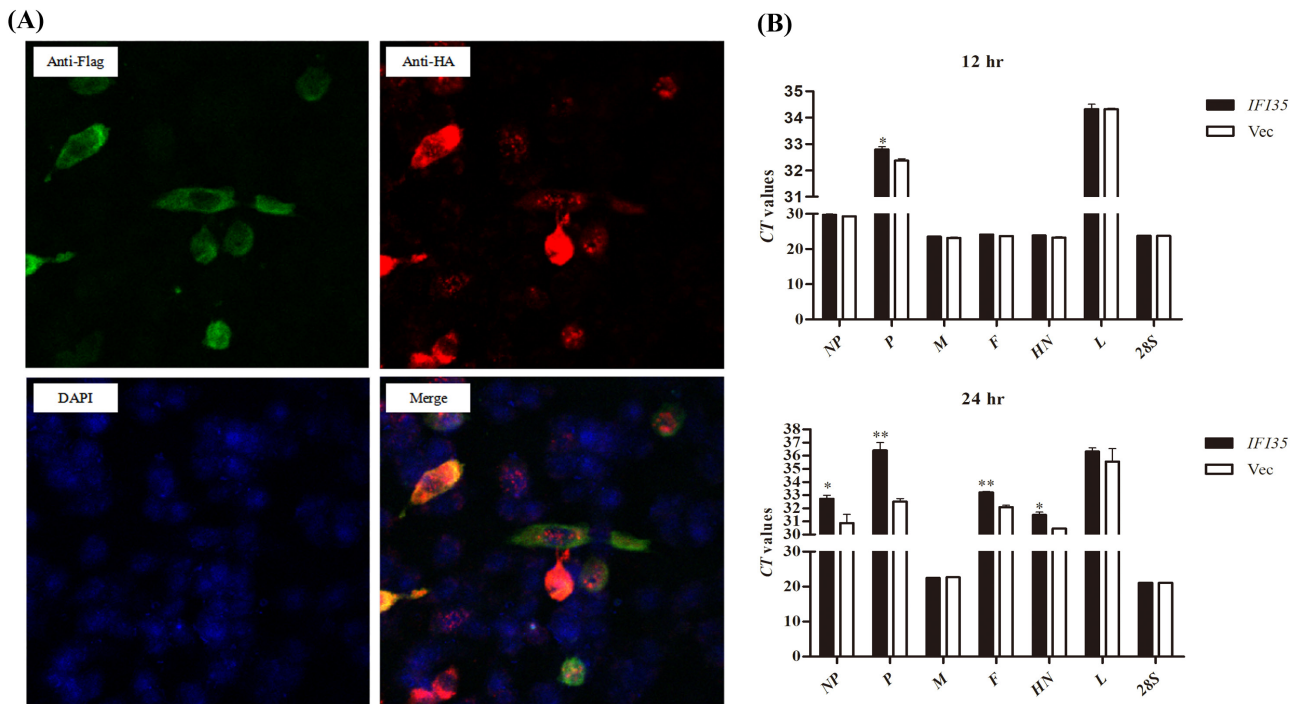


**Fig. 4.** Chicken interferon-induced protein-35 kDa (ChIFI35) affects viral gene transcription. (A) The plasmids pCAGGS-HA-P and pCAGGS-Flag-chIFI35 were co-transfected for 36 hr in DF-1 cells, and observed the cell sublocalization of chIFI35 and NDV P protein under the laser confocal microscopy (400 $\times$ ). (B) CT values of each viral gene transcript after F48E9 infection. Data are shown as the mean  $\pm$  SEM ( $n=3$ ). The statistical analysis was performed in GraphPad Prism using unpaired two-tailed  $t$ -tests: \* $P<0.05$ , \*\* $P<0.01$ .

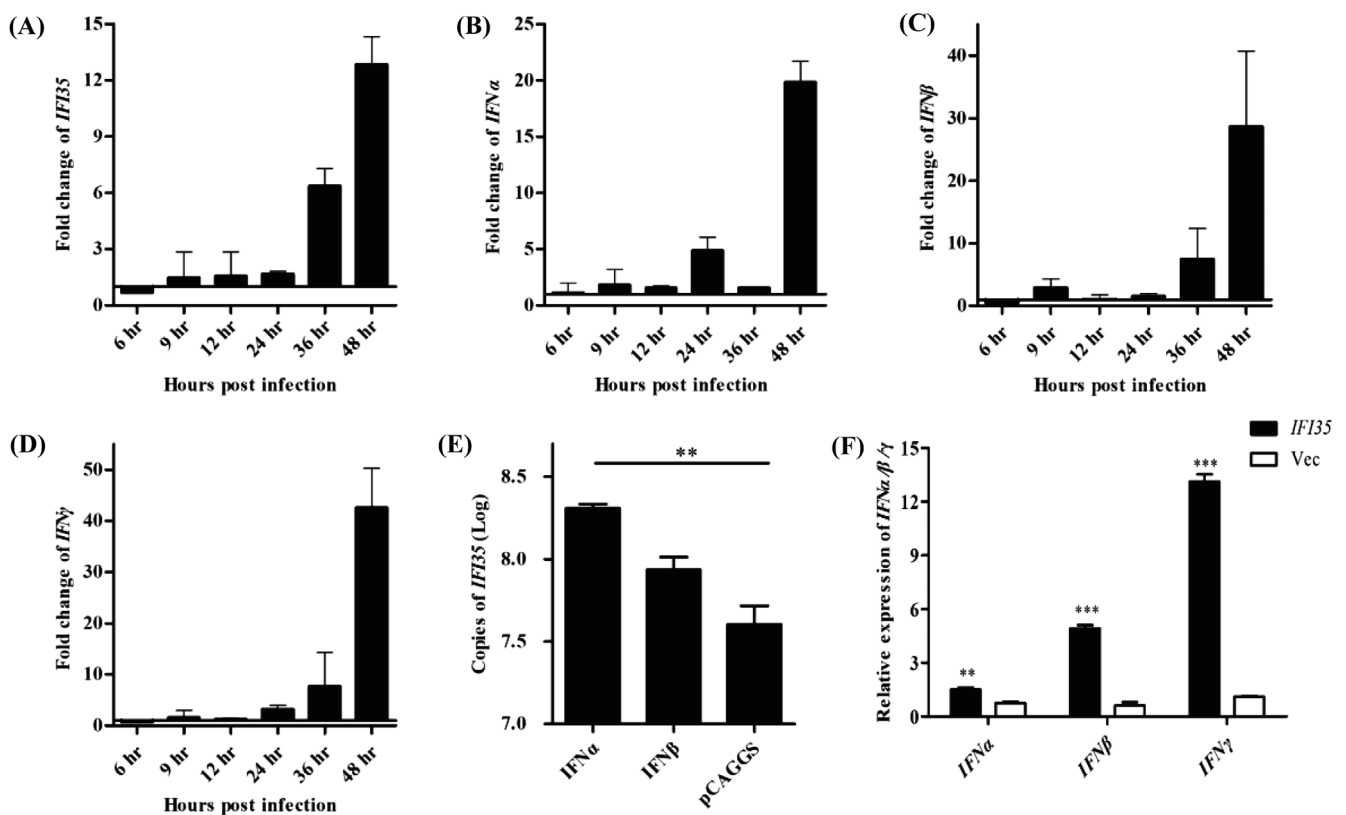


**Fig. 5.** Relative expression of chicken interferon-induced protein-35 kDa (chIFI35) and interferons (IFNs) during F48E9 infection. DF-1 cells were infected with F48E9 (0.1 moi, A–D), and the cells were collected at various timepoints to detect the expression changes using RT-qPCR of chIFI35 (A), *IFN $\alpha$*  (B), *IFN $\beta$*  (C), and *IFN $\gamma$*  (D). (E) ChIFI35 was increased by *IFN $\alpha$* /*IFN $\beta$*  over-expression. (F) *IFN $\alpha$* /*IFN $\beta$* /*IFN $\gamma$*  expression using RT-qPCR following transfection of DF-1 cells with chIFI35 and empty vector plasmids for 24 hr. Data are shown as the mean  $\pm$  SEM ( $n=3$ ). The statistical analysis was performed in GraphPad Prism using unpaired two-tailed  $t$ -tests: \*\* $P<0.01$ , \*\*\* $P<0.001$ .

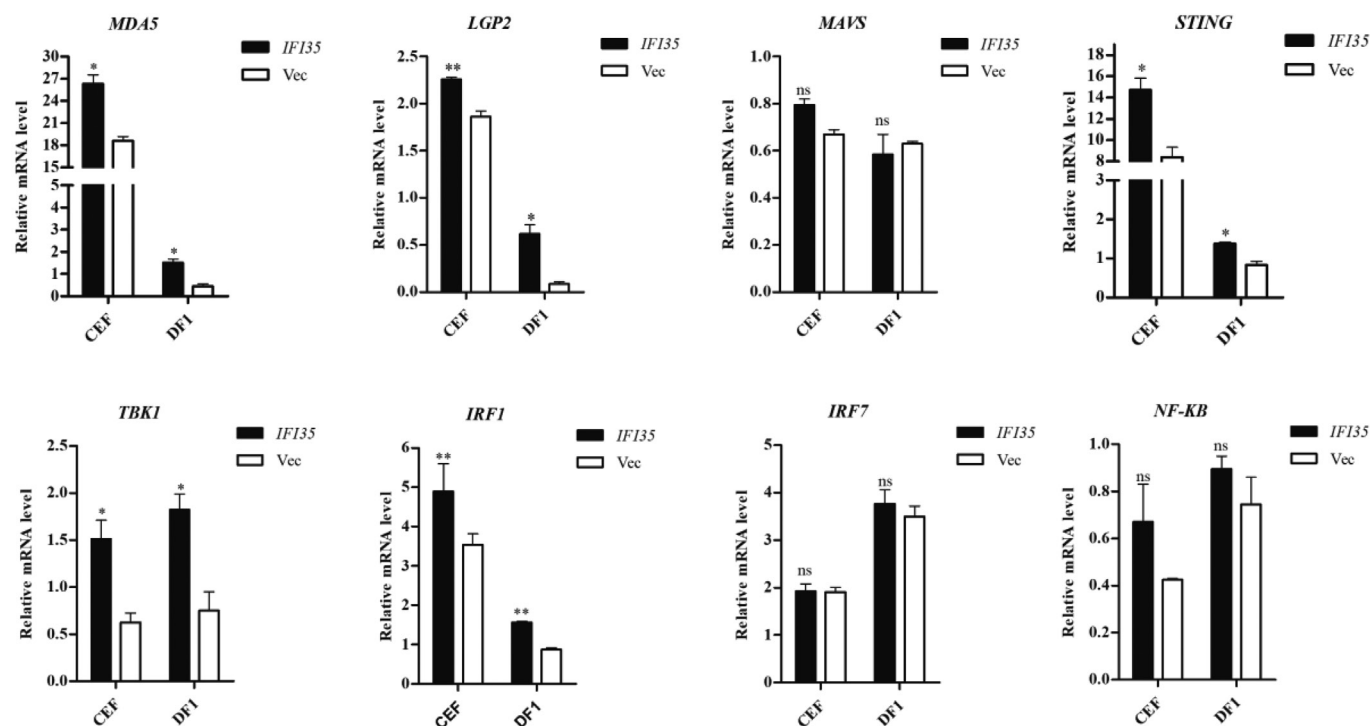


**Fig. 6.** Positive feedback regulation of interferon (IFN) expression by chicken interferon-induced protein-35 kDa (*IFI35*). After transfection with ch*IFI35* in DF-1 or CEF cells for 24 hr, cells were infected with F48E9 for a further 24 hr, and the *IFN* modulators were detected using RT-qPCR. Data are shown as the mean  $\pm$  SEM ( $n=3$ ). The statistical analysis was performed in GraphPad Prism using unpaired two-tailed *t*-tests: \* $P<0.05$ , \*\* $P<0.01$ .

## DISCUSSION

*IFI35* was first found in HeLa cells after interferon- $\gamma$  treatment in 1994 [1]. *IFI35* sequences have been reported in mouse, cattle, and fish [5, 18, 21]. To date, the pleiotropic effects of *IFI35* have not been examined in birds, with only limited reports in mammals and teleosts. In this study, the full-length ch*IFI35* cDNA was successfully cloned and sequenced for the first time. The ch*IFI35* protein consists two NID domains in the N-terminal, similar to human *IFI35* (hu*IFI35*) and rockfish *IFI35* (Rf*IFI35*) [18], suggesting that it interacts with Nmi protein to maintain stable and subcellular localization similar to hu*IFI35* or Rf*IFI35* [3]. In order to identify the evolutionary relationship between ch*IFI35* and other species, a neighbor-joining (NJ) tree was constructed, and which demonstrated that the amino acids sequences of *IFI35* were with high identity in birds, but with low identities to species in other four classes, which consistent with the amino acid sequences analysis. The pairwise alignment and phylogenetic analysis results showed that ch*IFI35* was homology among birds, suggesting similar structures and functions of it in birds.

Tissue distribution analysis revealed a broad tissue distribution of ch*IFI35* in healthy chickens. High lever expressions of ch*IFI35* were detected in the lung, proventriculus, brain, bursa of fabricius, kidney, and intestine. The rule of tissue distribution was similar to *IFI35* of fish and human [18]. Analysis ch*IFI35* expression in immune-associated tissues after F48E9 infection found that ch*IFI35* mRNA was high level expression in intestines, which was one of the major targets of velogenic NDV. Moreover, ch*IFI35* highly expressed in respiratory tract, lung and trache, as well as in the digestive tract, intestines, proventriculus, and gizzard. These tissues are the main targets of NDV and also present typical lesions of NDV infection. The viral loads of the trachea and kidney were slightly low, with slightly different from the expression of ch*IFI35*, which may be caused by the difference in inoculation method or sample collection time. Basically synchronized tissues distribution of ch*IFI35* and NDV suggests that ch*IFI35* involves in NDV infection process.

The current understanding of the role of *IFI35* in virus infections was limited. A previous study suggested that *IFI35* negatively regulates the innate immune signaling, and could promote VSV replication via keeping *RIG-I* in phosphorylated form and mediating proteasomal ubiquitination of *RIG-I* [5]. However, in this study, over-expression *IFI35* increased NDV, F48E9 and La Sota viral replication in DF-1 cells. This suggested that an anti-NDV infection role of ch*IFI35*, consistent with its reported role in against bovine foamy virus (BFV) [21] and foot-and-mouth disease virus (FMDV) [29]. The different roles of *IFI35* in VSV and NDV infection may cause by *RIG-I*. As well known, *RIG-I* was deficient in chicken [11]. Though *MDA5* replaced parts function of *RIG-I*, they are difference in response to viral infection and their final destiny (the way of degradation) [25].

Previous reports also demonstrated that ch*IFI35* could inhibit virus replication by interacting with viral structural proteins, such as the Btas protein of BFV [21]. Beside, *IFI35* could transfer into the nucleus from the cytoplasm and where it affects the virus

genome transcription or replication [21]. However, limited knowledge about *IFI35* in anti RNA virus infection has been revealed. In the current study, we identified a relationship between *chIFI35* and the transcription of NDV genes. Compared with the *CT* values of each viral gene between *chIFI35* over-expressing cells and vector-transfected cells, the *CT* values of *NP*, *P*, *F* and *HN* were significant increased, especially *P* gene, which indicates that *chIFI35* might affect the transcription of viral proteins in the viral genome. *NP* and *P* proteins are two important structural proteins and they compose the RNA-dependent RNA polymerase (RdRp) with the large (*L*) protein [8, 23]. The *F* and *HN* proteins are also two significant structural proteins that are mainly involved in viral invasion [23]. The subcellular location—determined using laser confocal microscopy—also showed that *chIFI35* co-localized with *P* protein in the cytoplasm. Those results suggested that *chIFI35* could affect the viral gene transcription, but the further research was needed to investigate the specific mechanism. Moreover, the nonstructural protein *V* was transcribed from *P* protein, which was considered as an antagonistic protein of *IFN* [2]. Here, the less transcripts of *P* gene could affect the expression of *V* protein, so as to result in decreasing the suppression of *IFN* from *V* protein.

*IFI35* was an interferon-induced protein and so we investigated the relationship between *chIFI35* expression and *IFNs*, and they have similar expression trends at different time points in F48E9-infected DF-1 cells, which was similar to *RfIFN-γ* and *RfIFI35* mRNA expression in fish [18]. However, we observed that *IFN-γ* expression induced by *IFI35* was apparently greater than that of type I *IFNs*, which indicated that the anti-NDV function of *chIFI35* may also depend on *IFN-γ*. NDV was considered an interferon inducer, especially type I, and we detected several upstream molecules of the interferon signaling pathways in uninfected or infected cells during *chIFI35* over-expression. We found that *chIFI35* could induce increased of the expression of *IFN* upstream molecules, including *MDA5*, *LGP2*, *STING*, *TBK1*, and *IRF1*, but have no significant changed in *MAVS*, *IRF7* and *NF-κB*. These data showed that *chIFI35* could induce *IFNs* and its regulator, which play an antiviral role in NDV replication. These results also indicated that *chIFI35* may play a significant role in the signal transmission of *IFN* production, similar to the result of *IFI35* in FMDV infection [29]. Unfortunately, the lack of chicken antibodies meant that we were unable to study the antiviral mechanism and protein levels in depth.

In summary, the present study identified and characterized *IFI35* in chicken and showed that this protein was conserved in birds. The highest expression of *chIFI35* mRNA was observed in the lung, followed by the brain and bursa of fabricius. *chIFI35* plays an important role in the antiviral NDV infection. The antiviral function of *chIFI35* may relate with that *chIFI35* induced *IFN* production and inhibited viral gene transcription. These data indicated that *chIFI35*'s anti-NDV action might be through multiple pathways.

CONFLICT OF INTEREST. The authors declare no conflict of interest.

ACKNOWLEDGMENTS. This work was funded by grants from the National Natural Science Foundation of China to Yang, Z.Q. (31572538) and Wang, X.L. (31672581), the Basic Natural Science Research Program of Shaanxi Province to Jia, Y.Q. (2021JQ-902), and the General Special Research Project of Department of Education of Shaanxi Province to Qiu, X.X. (20JK1003).

## REFERENCES

1. Bange, F. C., Vogel, U., Flohr, T., Kiekenbeck, M., Denecke, B. and Böttger, E. C. 1994. IFP 35 is an interferon-induced leucine zipper protein that undergoes interferon-regulated cellular redistribution. *J. Biol. Chem.* **269**: 1091–1098. [Medline] [CrossRef]
2. Chen, X., Jia, Y., Ren, S., Chen, S., Wang, X., Gao, X., Wang, C., Adam, F. E. A., Wang, X. and Yang, Z. 2020. Identification of Newcastle disease virus P-gene editing using next-generation sequencing. *J. Vet. Med. Sci.* **82**: 1231–1235. [Medline] [CrossRef]
3. Chen, J. and Naumovski, L. 2002. Intracellular redistribution of interferon-inducible proteins Nmi and IFP 35 in apoptotic cells. *J. Interferon Cytokine Res.* **22**: 237–243. [Medline] [CrossRef]
4. Chen, J., Shpall, R. L., Meyerdierts, A., Hagemeyer, M., Böttger, E. C. and Naumovski, L. 2000. Interferon-inducible Myc/STAT-interacting protein Nmi associates with IFP 35 into a high molecular mass complex and inhibits proteasome-mediated degradation of IFP 35. *J. Biol. Chem.* **275**: 36278–36284. [Medline] [CrossRef]
5. Das, A., Dinh, P. X., Panda, D. and Pattnaik, A. K. 2014. Interferon-inducible protein *IFI35* negatively regulates RIG-I antiviral signaling and supports vesicular stomatitis virus replication. *J. Virol.* **88**: 3103–3113. [Medline] [CrossRef]
6. Du, Y., Du, T., Shi, Y., Zhang, A., Zhang, C., Diao, Y., Jin, G. and Zhou, E. M. 2016. Synthetic Toll-like receptor 7 ligand inhibits porcine reproductive and respiratory syndrome virus infection in primary porcine alveolar macrophages. *Antiviral Res.* **131**: 9–18. [Medline] [CrossRef]
7. He, Y., Xie, Z., Dai, J., Cao, Y., Hou, J., Zheng, Y., Wei, T., Mo, M. and Wei, P. 2016. Responses of the Toll-like receptor and melanoma differentiation-associated protein 5 signaling pathways to avian infectious bronchitis virus infection in chicks. *Virol. Sin.* **31**: 57–68. [Medline] [CrossRef]
8. Hutcheson, J. M., Susta, L., Stice, S. L., Afonso, C. L. and West, F. D. 2015. Delayed Newcastle disease virus replication using RNA interference to target the nucleoprotein. *Biologicals* **43**: 274–280. [Medline] [CrossRef]
9. Irie, T., Kiyotani, K., Igarashi, T., Yoshida, A. and Sakaguchi, T. 2012. Inhibition of interferon regulatory factor 3 activation by paramyxovirus V protein. *J. Virol.* **86**: 7136–7145. [Medline] [CrossRef]
10. Jia, Y. Q., Wang, X. L., Wang, X. W., Yan, C. Q., Lv, C. J., Li, X. Q., Chu, Z. L., Adam, F. E. A., Xiao, S., Zhang, S. X. and Yang, Z. Q. 2018. Common microRNA mRNA Interactions in different Newcastle disease virus-infected chicken embryonic visceral tissues. *Int. J. Mol. Sci.* **19**: 1291. [CrossRef]
11. Kang, Y., Feng, M., Zhao, X., Dai, X., Xiang, B., Gao, P., Li, Y., Li, Y. and Ren, T. 2016. Newcastle disease virus infection in chicken embryonic fibroblasts but not duck embryonic fibroblasts is associated with elevated host innate immune response. *Virol. J.* **13**: 41. [Medline] [CrossRef]
12. Li, Y. P., Handberg, K. J., Juul-Madsen, H. R., Zhang, M. F. and Jørgensen, P. H. 2007. Transcriptional profiles of chicken embryo cell cultures following infection with infectious bursal disease virus. *Arch. Virol.* **152**: 463–478. [Medline] [CrossRef]

13. Li, Z., Luo, Q., Xu, H., Zheng, M., Abdalla, B. A., Feng, M., Cai, B., Zhang, X., Nie, Q. and Zhang, X. 2017. MiR-34b-5p suppresses melanoma differentiation-associated gene 5 (*MDA5*) signaling pathway to promote avian leukosis virus subgroup J (ALV-J)-infected cells proliferation and ALV-J replication. *Front. Cell. Infect. Microbiol.* **7**: 17. [[Medline](#)]
14. Nang, N. T., Lee, J. S., Song, B. M., Kang, Y. M., Kim, H. S. and Seo, S. H. 2011. Induction of inflammatory cytokines and Toll-like receptors in chickens infected with avian H9N2 influenza virus. *Vet. Res. (Faisalabad)* **42**: 64. [[Medline](#)] [[CrossRef](#)]
15. Livak, K. J. and Schmittgen, T. D. 2001. Analysis of relative gene expression data using real-time quantitative PCR and the 2(-Delta Delta C(T)) Method. *Methods* **25**: 402–408. [[Medline](#)] [[CrossRef](#)]
16. Liu, W. Q., Tian, M. X., Wang, Y. P., Zhao, Y., Zou, N. L., Zhao, F. F., Cao, S. J., Wen, X. T., Liu, P. and Huang, Y. 2012. The different expression of immune-related cytokine genes in response to velogenic and lentogenic Newcastle disease viruses infection in chicken peripheral blood. *Mol. Biol. Rep.* **39**: 3611–3618. [[Medline](#)] [[CrossRef](#)]
17. Nie, J., Liu, L., He, F., Fu, X., Han, W. and Zhang, L. 2013. CKIP-1: a scaffold protein and potential therapeutic target integrating multiple signaling pathways and physiological functions. *Ageing Res. Rev.* **12**: 276–281. [[Medline](#)] [[CrossRef](#)]
18. Perera, N. C. N., Godahewa, G. I., Nam, B. H. and Lee, J. 2016. Molecular structure and immune-stimulated transcriptional modulation of the first teleostean IFP35 counterpart from rockfish (*Sebastes schlegelii*). *Fish Shellfish Immunol.* **56**: 496–505. [[Medline](#)] [[CrossRef](#)]
19. Pomerantz, R. G., Mirvish, E. D., Erdos, G., Falo, L. D. Jr. and Geskin, L. J. 2010. Novel approach to gene expression profiling in Sézary syndrome. *Br. J. Dermatol.* **163**: 1090–1094. [[Medline](#)] [[CrossRef](#)]
20. Sutton, D., Aldous, E. W., Warren, C. J., Fuller, C. M., Alexander, D. J. and Brown, I. H. 2013. Inactivation of the infectivity of two highly pathogenic avian influenza viruses and a virulent Newcastle disease virus by ultraviolet radiation. *Avian Pathol.* **42**: 566–568. [[Medline](#)] [[CrossRef](#)]
21. Tan, J., Qiao, W., Wang, J., Xu, F., Li, Y., Zhou, J., Chen, Q. and Geng, Y. 2008. IFP35 is involved in the antiviral function of interferon by association with the viral tas transactivator of bovine foamy virus. *J. Virol.* **82**: 4275–4283. [[Medline](#)] [[CrossRef](#)]
22. Wang, X., Jia, Y., Ren, J., Liu, H., Adam, F. A., Wang, X. and Yang, Z. 2019. Insights into the chicken bursa of fabricius response to Newcastle disease virus at 48 and 72 hours post-infection through RNA-seq. *Vet. Microbiol.* **236**: 108389. [[Medline](#)] [[CrossRef](#)]
23. Wen, G., Shang, Y., Guo, J., Chen, C., Shao, H., Luo, Q., Yang, J., Wang, H. and Cheng, G. 2013. Complete genome sequence and molecular characterization of thermostable Newcastle disease virus strain TS09-C. *Virus Genes* **46**: 542–545. [[Medline](#)] [[CrossRef](#)]
24. Yin, R., Ding, Z., Liu, X., Mu, L., Cong, Y. and Stoeger, T. 2010. Inhibition of Newcastle disease virus replication by RNA interference targeting the matrix protein gene in chicken embryo fibroblasts. *J. Virol. Methods* **167**: 107–111. [[Medline](#)] [[CrossRef](#)]
25. Yu, Y., Huang, Y., Yang, Y., Wang, S., Yang, M., Huang, X. and Qin, Q. 2016. Negative regulation of the antiviral response by grouper LGP2 against fish viruses. *Fish Shellfish Immunol.* **56**: 358–366. [[Medline](#)] [[CrossRef](#)]
26. Yang, Y., Huang, Y., Yu, Y., Yang, M., Zhou, S., Qin, Q. and Huang, X. 2016. RING domain is essential for the antiviral activity of TRIM25 from orange spotted grouper. *Fish Shellfish Immunol.* **55**: 304–314. [[Medline](#)] [[CrossRef](#)]
27. Yang, C., Liu, F., Chen, S., Wang, M., Jia, R., Zhu, D., Liu, M., Sun, K., Yang, Q., Wu, Y., Chen, X. and Cheng, A. 2016. Identification of 2'-5'-oligoadenylate synthetase-like gene in goose: gene structure, expression patterns, and antiviral activity against Newcastle disease virus. *J. Interferon Cytokine Res.* **36**: 563–572. [[Medline](#)] [[CrossRef](#)]
28. Zhou, X., Liao, J., Meyerdierks, A., Feng, L., Naumovski, L., Bottger, E. C. and Omary, M. B. 2000. Interferon-alpha induces nmi-IFP35 heterodimeric complex formation that is affected by the phosphorylation of IFP35. *J. Biol. Chem.* **275**: 21364–21371. [[Medline](#)] [[CrossRef](#)]
29. Zheng, W., Li, X., Wang, J., Li, X., Cao, H., Wang, Y., Zeng, Q. and Zheng, S. J. 2014. A critical role of interferon-induced protein IFP35 in the type I interferon response in cells induced by foot-and-mouth disease virus (FMDV) protein 2C. *Arch. Virol.* **159**: 2925–2935. [[Medline](#)] [[CrossRef](#)]
30. Zhang, L., Tang, Y., Tie, Y., Tian, C., Wang, J., Dong, Y., Sun, Z. and He, F. 2007. The PH domain containing protein CKIP-1 binds to IFP35 and Nmi and is involved in cytokine signaling. *Cell. Signal.* **19**: 932–944. [[Medline](#)] [[CrossRef](#)]